imc-precip-iso: Open monthly stable isotope data of precipitation over the Indonesian Maritime Continent

R. Suwarman[1], S. H. S. Herho[2, 3, *], H. A. Belgaman[4], D. E. Irawan[5], K. Ichiyanagi[6], I. M. Yosa[1], A. I. D. Utami[7], S. Prayogo[8], and E. Aldrian[4]

[1]Atmospheric Science Research Group, Bandung Institute of Technology (ITB), Bandung, Indonesia
[2]Department of Earth and Planetary Sciences, University of California, Riverside, USA
[3]Department of Geology, University of Maryland, College Park, USA
[4]Research Center for Climate and Atmosphere (PRIMA) , National Research and Innovation Agency (BRIN), Bandung, Indonesia
[5]Applied Geology Research Group, Bandung Institute of Technology (ITB), Bandung, Indonesia
[6]Faculty of Advanced Science and Technology, Kumamoto University, Kumamoto, Japan
[7]Indonesian Meteorology, Climatology, and Geophysical Agency (BMKG), Jakarta, Indonesia
[8]Software Engineering Division, Manvis Teknologi Enjinering, Bandung, Indonesia
[*]Corresponding author: `sandy.herho@email.ucr.edu`

Abstract

Stable isotopes, δ^2H, δ^{18}O, and d-excess, are valuable tools as natural tracers of diffusion processes and phase changes in the global hydroclimatological cycle. The Indonesian Maritime Continent (IMC) is an archipelago area surrounded by very warm waters which induce convective activities as the primary heat source driving global atmospheric circulation. Given the central role of IMC in this hydroclimatological cycle, comprehensive study and data collection on the stable isotopes of precipitation in this region is crucial.

In this study, we collected monthly stable isotope data from 62 stations spread throughout the Indonesian archipelago from September 2010 to September 2017. We cleaned the data and conducted quality control activities by comparing the Local Meteoric Water Line (LMWL) to previous studies in a similar climatic region. We shared these data openly on our GitHub repository, making them easier to update and interact with users in the future.

1 Introduction

Indonesian Maritime Continent (IMC) comprises a group of islands surrounded by the Indian and Pacific Oceans. The region's climate is influenced by its insular geography and its position near the Equator. Located in the western part of the Indo-Pacific warm pool (IPWP), IMC is a source of latent heat release and deep convection which drives the Hadley and Walker cells, thus playing an essential role in the earth's hydrological cycle [1; 2]. IMC is also the only link for warmed surface waters from the Pacific Ocean to the Indian Ocean through the Indonesian Throughflow (ITF), a surface flow component of the global ocean conveyor belt (e. g. [3; 4; 5; 6; 7]).

In general, IMC experiences two seasons, namely the wet and dry seasons, each in boreal winter - spring (November-March/NDJFM) and boreal summer - fall (May - September/MJJAS) [8; 1]. During the wet season, there is warm sea surface temperature (SST) and heavy precipitation over the IMC, which is brought by the Asian winter monsoon, which is northeasterly to the north of the equator and northwesterly to the south of the equator, the opposite also happens in the dry season [9; 10; 1]. Besides the annual cycle, IMC precipitation is influenced by internal global atmosphere-ocean interactions, such as the El Niño Southern Oscillation (ENSO) (e. g. [11; 12; 13; 14; 15]) and the Indian Ocean Dipole mode (IOD) (e. g. [1; 16; 11; 17]). On an intra-annual scale, precipitation over the IMC is also influenced by the Madden-Julian Oscillation (MJO), which propagates from the Indian Ocean to the Pacific Ocean via IMC (e. g. 18; 19; 11; 20; 21; 22).

Given the importance of IMC in understanding the earth's hydroclimatological phenomena (23), investigation of precipitation characteristics is inevitable. One of the characteristics of precipitation that is important to investigate is the traditional water-stable isotopes of precipitation (δ^{18}O and δ^{2}H) which are considered one of the natural tracers of hydrological cycles as a consequence of equilibrium and kinetic processes during phase transitions and diffusive processes (24; 25; 26; 27). In general, oxygen-18 (δ^{18}O) and deuterium (δ^{2}H) at mid- and high-latitudes are correlated with temperature (e. g. 28; 29; 30; 31; 32). However, in tropical regions such as the IMC, these two isotopic compositions show a negative correlation (e.g. 33; 34; 35; 36) due to a rainout process known as the amount effect (37). δ^{18}O can also be used as a signature of the water vapour transport process during ENSO and MJO over the IMC (38; 39; 40). Observations of δ^{18}O and δ^{2}H in the tropics are also crucial to confirm the sensitivity of proxy precipitation observations in paleoclimatology using proxy system modelling (PSM), which requires modern precipitation isotope data in the region (41). Modern precipitation isotope observations are also needed to correct calculations performed by isotope-enabled General Circulation Models (iGCMs) (e. g. 42; 43; 44; 45).

Until recently, there is not much open and publicly accessible data on traditional precipitation isotope over the IMC. There are four isotope stations operated by the International Atomic Energy Agency (IAEA) within the framework of the Global Network of Isotopes in Precipitation (GNIP) program. However, these stations stopped operating in 2003 and only cover the Java region, except for the Jayapura station in Papua (46). In addition, there were isotope observations conducted by the Institute of Observational Research for Global Change (IORGC)/Japan Agency for Marine-Earth Science and Technology (JAMSTEC) conducted at six stations across IMC between 2001 and 2007 (33; 46).

In this study, we conducted monthly δ^{18}O and δ^{2}H sampling at 62 observation stations along the IMC from September 2010 to September 2017. Part of these data (30 stations) have been used in a study by Belgaman et al. (47) but has yet to be opened to the public. We opened the δ^{18}O and δ^{2}H measurements to the public on our GitHub repository to support democratizing knowledge based on open-source code and reproducible datasets (48).

2 Material and Methods

2.1 Data Acquisition

We conducted field sampling from 62 meteorological and climatological stations owned by the Indonesian Meteorology, Climatology, and Geophysical Agency (BMKG) throughout the IMC area (Figure 1). To find out the details of station numbering and their location, see the table on the following URL: `https://github.com/sandyherho/imc-precip-iso/blob/main/output_data/sta_list.csv`. We collected these precipitation samples manually using buckets and then put them into 6 mL glass vials with screw caps. We collected this monthly precipitation samples from September 2010 to September 2017.

We measured δ^{18}O and δ^{2}H using the Picarro® L2120-i instrument using the cavity ring-down spectroscopy technique, which has proven practical and accurate in measuring water isotopes (e. g. 51; 52; 53; 54; 55). We measured the ratio of the abundance of the heavy to light isotopes (R), in the context of this study, ^{2}H/^{1}H and ^{18}O/^{16}O, from samples by comparing them to the international standard, namely the Vienna Standard Mean Ocean Water (VSMOW) (56) so that δ values were obtained in units per mil (‰) using the following equation:

$$\delta = \left(\frac{R_{\text{sample}}}{R_{\text{standard}}} - 1 \right) \times 10^{3} \tag{1}$$

Due to the limited supply of international standards (is), we calibrated the samples (x) using three working standards (ws), Aqua Standard®, SLW2 and ICE2, which had been calibrated against VSMOW. This calculation process is formulated through the following equation (57):

$$\delta_{x-is} = \delta_{x-ws} + \delta_{ws-is} + (\delta_{x-ws} \times \delta_{ws-is}) \times 10^{-3} \tag{2}$$

Long-term standard errors (1σ) for these δ^{18}O and δ^{2}H measurements are ± 0.08 ‰ and ± 0.22 ‰, respectively (47).

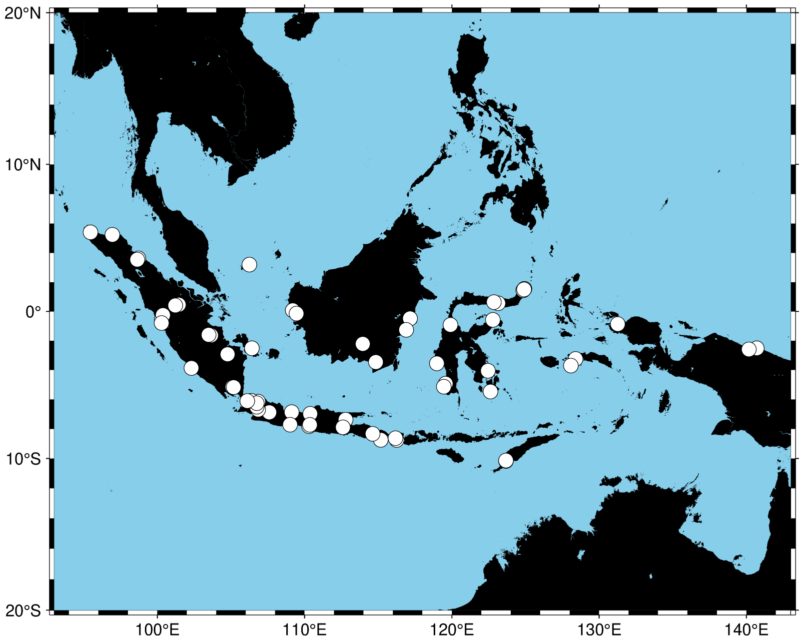

Figure 1: Location of the stations at which monthly samples of precipitation were collected for isotope measurements over the IMC (rendered using **PyGMT** (49; 50)).

2.2 Data Wrangling

Microsoft® Excel files extracted from the isotope measurement instrument were then converted into a text-formatted files, i. e. comma-separated values (CSV) format to make them easier to read by various kinds of software without being limited by a paid license (58; 59). These data were then splitted into time series for each station and the entire IMC. In addition, we also calculated d-excess (d), which is defined as the deviation from δ^2H to δ^{18}O according to the definition of the Global Meteoric Water Line (GMWL) (60), which can be written as follows:

$$d = \delta^2\text{H} - 8\delta^{18}\text{O} \tag{3}$$

Calculation of this d-excess is necessary, given its correlation with the oceanic source of precipitation (61; 28). Globally, this d-excess is a dependent variable of the relative humidity of the sea surface (62). Using d-excess, we can find the moisture flux anomaly during extreme events, such as ENSO influences in precipitation (e. g. 63; 64; 65). We did the entire data wrangling process using **NumPy** (66) and **pandas** (67) libraries in the Python computing environment.

2.3 Local Meteoric Water Line (LMWL) Estimation

We performed Local Meteoric Water Line (LMWL) calculations as part of our quality control efforts. It has been known since a study conducted by Craig (60) that there is a linear relationship between δ^2H to δ^{18}O globally, which can be formulated as follows:

$$\delta^2\text{H} = 8\delta^{18}\text{O} + 10 \tag{4}$$

However, local slope variations and intercepts were only discovered after collecting IAEA/GNIP observations through the study of Rozanski et al. (68), better known as LMWL. In this study, it is emphasized that the relationship between the two isotopes is still linear. Variations in the slope may store information about the local seasonal climatology (69).

We used Bayesian Linear Regression (BLR) to determine the relationship between δ^2H and δ^{18}O over the IMC. BLR allows better handling of uncertainty in models. This method recognizes that we need perfect information about model parameters or data variability. We can represent this uncertainty using a probability distribution on the parameters in the Bayesian approach. This approach helps generate more realistic and credible parameter estimates and confidence intervals. The BLR approach allows us to incorporate any prior knowledge about the model parameters. This is useful when we need more data or want to use existing domain knowledge. In this study, we determined the priors for slopes and intercepts from the global data compilation for humid tropical regions (Köppen class A) that was done by Putman et al. (69). Apart from single-point estimates (as in "frequentist" linear regression), the BLR gives a full posterior distribution of model parameters after looking at the data. This provides richer information about the parameter uncertainties and allows for more robust modelling of the δ^2H - δ^{18}O covariance. Because of these advantages, the Bayesian approaches have recently been popular for solving water isotope problems (e. g. 69; 70; 71; 72; 73; 74; 75). The full benefits of using BLR can be found in Klauenberg et al. (76).

The simple linear regression model that we used to explain the statistical relationship between δ^2H and δ^{18}O is illustrated in the following equation:

$$\delta^2\text{H}_i = \beta_0 + \beta_1 \delta^{18}\text{O}_i + \varepsilon_i \tag{5}$$

, where $\delta^2\text{H}_i$ and $\delta^{18}\text{O}_i$ are the observed deuterium and oxygen-18 isotope values for the $i-$th data point, respectively. β_0 and β_1 are the unknown regression coefficients (intercept and slope) to be estimated. ε_i is the random error term, assumed to be normally distributed, with mean zero and constant variance σ^2.

BLR estimation started by specifying the prior distributions for the unknown parameters: β_0, β_1, and σ^2. In this study, we assumed normal prior for intercept and slope, and uniform prior for variance (77):

$$\begin{cases} \beta_0 \sim \mathcal{N}\left(m_0, s_0^2\right) \\ \beta_1 \sim \mathcal{N}\left(m_1, s_1^2\right) \\ \sigma^2 \sim U(a, b) \end{cases} \tag{6}$$

Parameters m_0, m_1, s_0, s_1, a, and b were determined from the global observation database for the humid tropical regions (Köppen class A) (69).

Assuming errors ε_i are normally distributed, the likelihood function can be written in the following form:

$$p\left(\delta^2\text{H}_i|\beta_0, \beta_1, \delta^{18}\text{O}_i, \sigma^2\right) = \frac{1}{\sqrt{2\pi\sigma^2}} \exp\left(-\frac{\left(\delta^2\text{H}_i - \beta_0 - \beta_1 - \delta^{18}\text{O}_i\right)^2}{2\sigma^2}\right) \tag{7}$$

The joint posterior distribution of the BLR parameters given the observed isotope data $\left(\delta^2\text{H}_i, \delta^{18}\text{O}_i\right)$ is:

$$p(\beta_0, \beta_1, \sigma^2|\text{data}) \propto p(\text{data}|\beta_0, \beta_1, \sigma^2) \times p(\beta_0) \times p(\beta_1) \times p(\sigma^2) \tag{8}$$

, where $p(\text{data}|\beta_0, \beta_1, \sigma^2)$ is the likelihood and $p(\beta_0)$, $p(\beta_1)$, and $p(\sigma^2)$ are the priors.

We used a simple algorithm from the Markov chain Monte Carlo (MCMC) methods (78), the Metropolis-Hastings (MH) algorithm (79; 80), to estimate the posterior distribution. This algorithm can approximate the posterior distribution without the need to compute the normalization constant (81). MH algorithm has also proven reliable enough to be used in hydroclimatological problems (e. g. 69; 82; 83; 84; 85; 86; 87; 88). MH algorithm can be summarized into several steps as follows:

1. Intitialize the parameters $\beta_0^{(0)}$, $\beta_1^{(0)}$, and $\sigma_0^{2(0)}$ to some initial values.
2. For iteration $t = 1$ to T, where T is the number of iterations (in this study, we used 10,000 steps with the tuning of 2,000 steps which are the "burn in" iterations used to accelerate convergence (78; 89)):
   (a) Calculate the acceptance ratio α:

$$\alpha = \frac{p(\text{data}|\beta_0, \beta_1, \sigma^{2*}) \times p(\beta_0) \times p(\beta_1) \times p(\sigma^{2*})}{p(\text{data}|\beta_0^{(t-1)}, \beta_1^{(t-1)}, \sigma^{2(t-1)}) \times p(\beta_0^{(t-1)}) \times p(\beta_1^{(t-1)}) \times p(\sigma^{2(t-1)})} \tag{9}$$

   (b) Generate a uniform random number u from $[0, 1]$.

   (c) If $u < \alpha$, accept the proposed parameters: $\beta_0^{(t)} = \beta_0$, $\beta_1^{(t)} = \beta_1$, $\sigma^{2(t)} = \sigma^{2*}$. Otherwise, keep the previous parameters: $\beta_0^{(t)} = \beta_0^{(t-1)}$, $\beta_1^{(t)} = \beta_1^{(t-1)}$, $\sigma^{2(t)} = \sigma^{2(t-1)}$.

3. After T iterations, we have samples from the posterior distribution. We use these samples to estimate the posterior mean, credible intervals, and other properties of the parameters.

This study uses a symmetrical Gaussian proposal distribution to simplify computing the acceptance ratio (78; 90; 89; 91). We implemented the entire BLR process using the **PyMC3** library within the Python computing environment (92).

3 Results and Discussion

The number of data points at each isotope observation station can be seen in Figure 2. The three stations with the most data collection were the Kemayoran Air Pollution Post in Jakarta (#1), with a total of 47 data points, followed by Deli Serdang in North Sumatra (#5) with a total of 46 data points, and in third place is the Bengkulu station (#11) which is located on the southwest coast of Sumatra with a total of 43 observations of data points. The stations with the fewest number of observations include Tambang (#57), located in Riau, and Ranomeeto (#58) in Southeast Sulawesi, each with two data points. Stations with the second-fewest number of observations include El Tari (#24) and Kupang in East Nusa Tenggara (#38), Mlati (#49) in Sleman, Yogyakarta, Malikusaleh (#53) in North Aceh, Koba (#56) in Bangka Belitung, each of which recorded only three data points. The stations with the third-fewest number of observations are Tarempa (#36) in the Riau Archipelago, West Seram (#48) in Maluku, and Sorong (#54) in Southwest Papua, each of which only has four data points. All stations' average and median data points were 21.968 and 22, respectively. These are very small because only about a quarter of the 85 months of observation period had successfully extracted δ^2H and δ^{18}O values.

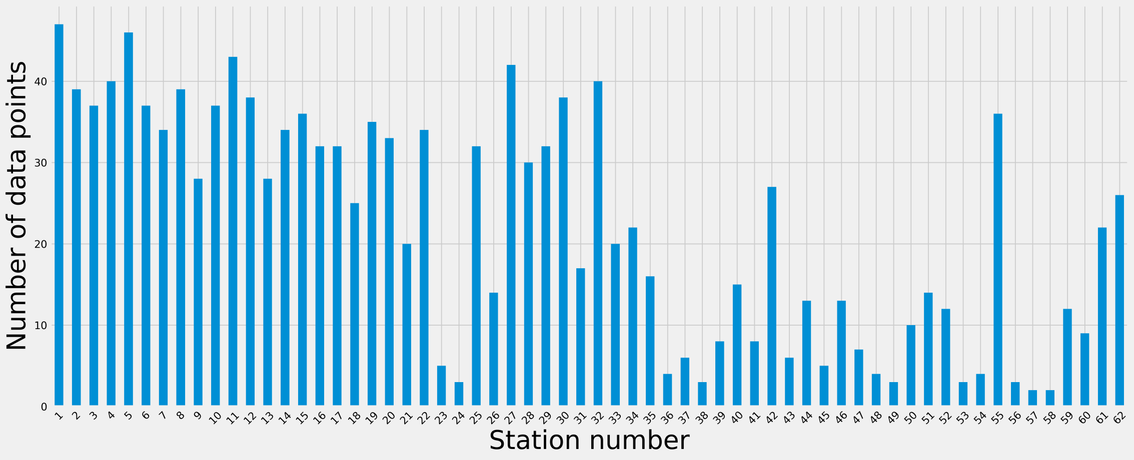

Figure 2: Availability of data points at each isotope station over the IMC collected in this study.

Weaknesses in data collection are also found in the need for more coverage of areas outside parts of Sumatra and Java due to limited access to transportation for sending samples. This must be underlined because most of the isotope measurements we produced in this study are concentrated in a region with monsoonal rainfall classifications (8; 93; 94). In contrast, anti-monsoonal and semi-annual regions are underrepresented. This is also evident in the less distribution of δ^2H and δ^{18}O values at stations in these two regions, as shown in the boxplots in Figure 3.

By combining δ^2H and δ^{18}O from all stations, we performed BLR inference, where the results of trace plots and the posterior distribution of the linear regression parameters can be seen in Figure 4. There is a convergence of all linear regression parameters, which can be visually seen in the trace plots (Figure 4a). The posterior distribution of the LMWL parameters that have been calculated using the MH algorithm is shown in Figure 4b. The mean and standard deviation of the posterior intercept are 3.506 ‰ and 1.732 ‰, respectively. Meanwhile, the mean and standard deviation of the posterior slope are 7.298 ‰ and 0.267 ‰, respectively. Then, for a 2σ credible interval, we can write the LMWL equation as follows:

$$\delta^2\text{H} = 7.298(\pm 0.534)\delta^{18}\text{O} + 3.506(\pm 3.464) \tag{10}$$

The two regression coefficients in Equation 10 are shallower when compared to GMWL. This indicates the occurrence of a sub-cloud evaporation process which indicates the occurrence of re-evaporation from rainwater after falling under the clouds through a tropical convective processes. Visually this can be seen by shifting the LMWL regression line clockwise when compared to the GMWL (Figure 5). Similar things were also found in previous studies over the Maritime Continent (95; 96; 26).

4 Conclusion

Based on water isotope observations from 62 stations that we collected from September 2010 to September 2017, we managed to build monthly δ^2H, δ^{18}O, and d-excess datasets per station and for all IMC, which are shared openly, accessible, and easily updated on the GitHub repository. We have also performed quality control on these data by calculating the LMWL using BLR, which is under the range of slopes and intercepts in previous studies conducted in areas with similar climate types (e. g. 95; 96; 69; 26). The open data we shared are by far the most complete data over the IMC for stable isotopes of precipitation.

There are limitations to this study. One of them is that we should have checked the amount effect. This is due to the limitation of station precipitation data, which contains many empty data. In the future, a combination of station data and other high-resolution data sources is needed, such as the Climate Hazards Group InfraRed Precipitation with Station data (CHIRPS) (97), which can be used to calculate the amount effect. In addition, this monthly water isotope observation activities over the IMC were stopped in September 2017. This activity should be continued, given the central position of the IMC in the Earth's climate system, which is currently undergoing significant changes as a consequence of the unprecedented increase in anthropogenic radiative forcing. The study of water isotopes in precipitation over the IMC can undoubtedly deepen our understanding of anthropogenic and natural attributions in the hydrologic cycle in the tropics.

Acknowledgments

We are grateful to Michael N. Evans (UMD) for discussing fractionation on precipitation isotopes in the tropics, which was useful in producing these data. This study was supported by ITB Research, Community Service and Innovation Program (PPMI-ITB) and Japan Society for the Promotion of Science (JSPS) KAKENHI (#24510256 and #16H05619). Open-source code and publicly available data can be accesed from: `https://github.com/sandyherho/imc-precip-iso/`.

References

[1] S. Yang, T. Zhang, Z. Li, and S. Dong, "Climate variability over the maritime continent and its role in global climate variation: A review," *Journal of Meteorological Research*, vol. 33, no. 6, pp. 993–1015, 2019.

[2] P. Xue, P. Malanotte-Rizzoli, J. Wei, and E. A. B. Eltahir, "Coupled ocean-atmosphere modeling over the Maritime Continent: A review," *Journal of Geophysical Research: Oceans*, vol. 125, no. 6, p. e2019JC014978, 2020.

[3] J. S. Godfrey, "The effect of the Indonesian throughflow on ocean circulation and heat exchange with the atmosphere: A review," *Journal of Geophysical Research: Oceans*, vol. 101, no. C5, pp. 12217–12237, 1996.

[4] M. Li, A. L. Gordon, L. K. Gruenburg, J. Wei, and S. Yang, "Interannual to decadal response of the Indonesian throughflow vertical profile to Indo-Pacific forcing," *Geophysical Research Letters*, vol. 47, no. 11, p. e2020GL087679, 2020.

[5] S. Makarim, J. Sprintall, Z. Liu, W. Yu, A. Santoso, X.-H. Yan, and R. D. Susanto, "Previously unidentified Indonesian Throughflow pathways and freshening in the Indian Ocean during recent decades," *Scientific Reports*, vol. 9, no. 1, p. 7364, 2019.

[6] T. Nagai, T. Hibiya, and F. Syamsudin, "Direct estimates of turbulent mixing in the Indonesian archipelago and its role in the transformation of the Indonesian throughflow waters," *Geophysical Research Letters*, vol. 48, no. 6, p. e2020GL091731, 2021.

[7] A. Santoso, M. H. England, J. B. Kajtar, and W. Cai, “Indonesian Throughflow Variability and Linkage to ENSO and IOD in an Ensemble of CMIP5 Models,” *Journal of Climate*, vol. 35, no. 10, pp. 3161–3178, 2022.

[8] E. Aldrian and R. D. Susanto, “Identification of three dominant rainfall regions within Indonesia and their relationship to sea surface temperature,” *International Journal of Climatology*, vol. 23, no. 12, pp. 1435–1452, 2003.

[9] C.-P. Chang, P. A. Harr, and H.-J. Chen, “Synoptic disturbances over the equatorial South China Sea and western Maritime Continent during boreal winter,” *Monthly Weather Review*, vol. 133, no. 3, pp. 489–503, 2005.

[10] C.-P. Chang, Z. Wang, J. McBride, and C.-H. Liu, “Annual cycle of Southeast Asia—Maritime Continent rainfall and the asymmetric monsoon transition,” *Journal of Climate*, vol. 18, no. 2, pp. 287–301, 2005.

[11] S. C. Peatman, J. Schwendike, C. E. Birch, J. H. Marsham, A. J. Matthews, and G.-Y. Yang, “A local-to-large scale view of Maritime Continent rainfall: Control by ENSO, MJO, and equatorial waves,” *Journal of Climate*, vol. 34, no. 22, pp. 8933–8953, 2021.

[12] J. Zhu, Z. Guan, and X. Wang, “Variations of Summertime SSTA Independent of ENSO in the Maritime Continent and Their Possible Impacts on Rainfall in the Asian–Australian Monsoon Region,” *Journal of Climate*, vol. 35, no. 24, pp. 7949–7964, 2022.

[13] C. Chen, S. Sahany, A. F. Moise, X. R. Chua, M. E. Hassim, G. Lim, and V. Prasanna, “ENSO–Rainfall Teleconnection over the Maritime Continent Enhances and Shifts Eastward under Warming,” *Journal of Climate*, vol. 36, no. 14, pp. 4635–4663, 2023.

[14] C. Gao and G. Li, “Asymmetric effect of enso on the maritime continent precipitation in decaying summers,” *Climate Dynamics*, vol. 61, p. 2839–2852, 2023.

[15] J. Lu, T. Li, and X. Shen, “Precipitation diurnal cycle over the maritime continent modulated by ENSO,” *Climate Dynamics*, vol. 61, p. 2547–2564, 2023.

[16] C. Hu, T. Lian, H.-N. Cheung, S. Qiao, Z. Li, K. Deng, S. Yang, and D. Chen, “Mixed diversity of shifting IOD and El Niño dominates the location of Maritime Continent autumn drought,” *National Science Review*, vol. 7, no. 7, pp. 1150–1153, 2020.

[17] H.-M. Xiao, M.-H. Lo, and J.-Y. Yu, “The increased frequency of combined El Niño and positive IOD events since 1965s and its impacts on maritime continent hydroclimates,” *Scientific Reports*, vol. 12, no. 1, p. 7532, 2022.

[18] M.-S. Ahn, D. Kim, Y.-G. Ham, and S. Park, “Role of Maritime Continent land convection on the mean state and MJO propagation,” *Journal of Climate*, vol. 33, no. 5, pp. 1659–1675, 2020.

[19] Y. Wei, Z. Pu, and C. Zhang, “Diurnal cycle of precipitation over the Maritime Continent under modulation of MJO: Perspectives from cloud-permitting scale simulations,” *Journal of Geophysical Research: Atmospheres*, vol. 125, no. 13, p. e2020JD032529, 2020.

[20] H. Bai and C. Schumacher, “Topographic influences on diurnally driven MJO rainfall over the Maritime Continent,” *Journal of Geophysical Research: Atmospheres*, vol. 127, no. 6, p. e2021JD035905, 2022.

[21] S. Abhik, H. H. Hendon, and C. Zhang, “The Indo-Pacific Maritime Continent Barrier Effect on MJO Prediction,” *Journal of Climate*, vol. 36, no. 3, pp. 945–957, 2023.

[22] J. Hudson and E. Maloney, “The Role of Surface Fluxes in MJO Propagation through the Maritime Continent,” *Journal of Climate*, vol. 36, no. 6, pp. 1633–1652, 2023.

[23] M. D. Yamanaka, “Physical climatology of Indonesian maritime continent: An outline to comprehend observational studies,” *Atmospheric Research*, vol. 178, pp. 231–259, 2016.

[24] F. Tritschler, M. Binder, F. Händel, D. Burghardt, P. Dietrich, and R. Liedl, “Collected Rain Water as Cost-Efficient Source for Aquifer Tracer Testing,” *Groundwater*, vol. 58, no. 1, pp. 125–131, 2020.

[25] S. Valdivielso, E. Vázquez-Suñé, and E. Custodio, “Origin and variability of oxygen and hydrogen isotopic composition of precipitation in the Central Andes: A review,” *Journal of Hydrology*, vol. 587, p. 124899, 2020.

[26] S. He, D. Jackisch, D. Samanta, P. K. Y. Yi, G. Liu, X. Wang, and N. F. Goodkin, "Understanding tropical convection through triple oxygen isotopes of precipitation from the maritime continent," *Journal of Geophysical Research: Atmospheres*, vol. 126, no. 4, p. e2020JD033418, 2021.

[27] F. Malik, S. Butt, and N. Mujahid, "Variation in isotopic composition of precipitation with identification of vapor source using deuterium excess as tool," *Journal of Radioanalytical and Nuclear Chemistry*, pp. 1–8, 2022.

[28] J. Bershaw, "Controls on deuterium excess across Asia," *Geosciences*, vol. 8, no. 7, p. 257, 2018.

[29] J. Y. Liu, F. P. Zhang, Q. Feng, Y. F. Wei, L. H. Huang, Z. X. Li, S. Nie, and L. Li, "Stable isotopes characteristics of precipitation over shaanxi-gansu-ningxia and its water vapor sources," *The Journal of Applied Ecology*, vol. 30, no. 7, pp. 2191–2200, 2019.

[30] C. C. Routson, N. P. McKay, D. S. Kaufman, M. P. Erb, H. Goosse, B. N. Shuman, J. R. Rodysill, and T. Ault, "Mid-latitude net precipitation decreased with Arctic warming during the Holocene," *Nature*, vol. 568, no. 7750, pp. 83–87, 2019.

[31] C. C. Xia, K. Chen, J. Zhou, J. Mei, Y. P. Liu, and G. D. Liu, "Comparison of precipitation stable isotopes during wet and dry seasons in a subtropical monsoon climate region of China," *Applied Ecology & Environmental Research*, vol. 17, no. 5, 2019.

[32] C. Xia, G. Liu, K. Chen, Y. Hu, J. Zhou, Y. Liu, and J. Mei, "Stable isotope characteristics for precipitation events and their responses to moisture and environmental changes during the summer monsoon period in southwestern china.," *Polish Journal of Environmental Studies*, vol. 29, no. 3, 2020.

[33] N. Kurita, K. Ichiyanagi, J. Matsumoto, M. D. Yamanaka, and T. Ohata, "The relationship between the isotopic content of precipitation and the precipitation amount in tropical regions," *Journal of Geochemical Exploration*, vol. 102, no. 3, pp. 113–122, 2009.

[34] N. C. Munksgaard, N. Kurita, R. Sánchez-Murillo, N. Ahmed, L. Araguas, D. L. Balachew, M. I. Bird, S. Chakraborty, N. K. Chinh, K. M. Cobb, *et al.*, "Data descriptor: Daily observations of stable isotope ratios of rainfall in the tropics," *Scientific reports*, vol. 9, no. 1, p. 14419, 2019.

[35] C. Xia, G. Liu, J. Mei, Y. Meng, W. Liu, and Y. Hu, "Characteristics of hydrogen and oxygen stable isotopes in precipitation and the environmental controls in tropical monsoon climatic zone," *International Journal of Hydrogen Energy*, vol. 44, no. 11, pp. 5417–5427, 2019.

[36] D. Jackisch, B. X. Yeo, A. D. Switzer, S. He, D. L. M. Cantarero, F. P. Siringan, and N. F. Goodkin, "Precipitation stable isotopic signatures of tropical cyclones in Metropolitan Manila, Philippines, show significant negative isotopic excursions," *Natural Hazards and Earth System Sciences*, vol. 22, no. 1, pp. 213–226, 2022.

[37] W. Dansgaard, "Stable isotopes in precipitation," *Tellus*, vol. 16, no. 4, pp. 436–468, 1964.

[38] R. Suwarman, K. Ichiyanagi, M. Tanoue, K. Yoshimura, S. Mori, M. D. Yamanaka, N. Kurita, and F. Syamsudin, "The variability of stable isotopes and water origin of precipitation over the Maritime Continent," *SOLA*, vol. 9, pp. 74–78, 2013.

[39] H. A. Belgaman, K. Ichiyanagi, M. Tanoue, R. Suwarman, K. Yoshimura, S. Mori, N. Kurita, M. D. Yamanaka, and F. Syamsudin, "Intraseasonal variability of δ18O of precipitation over the Indonesian maritime continent related to the Madden–Julian oscillation," *SOLA*, vol. 12, pp. 192–197, 2016.

[40] R. Suwarman, K. Ichiyanagi, M. Tanoue, K. Yoshimura, S. Mori, M. D. Yamanaka, F. Syamsudin, and H. A. Belgaman, "El niño southern oscillation signature in atmospheric water isotopes over maritime continent during wet season," *Journal of the Meteorological Society of Japan. Ser. II*, vol. 95, no. 1, pp. 49–66, 2017.

[41] M. N. Evans, S. E. Tolwinski-Ward, D. M. Thompson, and K. J. Anchukaitis, "Applications of proxy system modeling in high resolution paleoclimatology," *Quaternary Science Reviews*, vol. 76, pp. 16–28, 2013.

[42] P. Peng, X. J. Zhang, and J. Chen, "Bias correcting isotope-equipped GCMs outputs to build precipitation oxygen isoscape for eastern China," *Journal of Hydrology*, vol. 589, p. 125153, 2020.

[43] Y. Nan, Z. He, F. Tian, Z. Wei, and L. Tian, "Can we use precipitation isotope outputs of isotopic general circulation models to improve hydrological modeling in large mountainous catchments on the Tibetan Plateau?," *Hydrology and Earth System Sciences*, vol. 25, no. 12, pp. 6151–6172, 2021.

[44] J. Chen, J. Chen, X. J. Zhang, P. Peng, and C. Risi, "A 148-year precipitation oxygen isoscape for China generated based on data fusion and bias correction of iGCMs simulations," *Earth System Science Data Discussions*, pp. 1–27, 2022.

[45] J. Chen, J. Chen, X. J. Zhang, P. Peng, and C. Risi, "A century and a half precipitation oxygen isoscape for China generated using data fusion and bias correction," *Scientific Data*, vol. 10, no. 1, p. 185, 2023.

[46] H. A. Belgaman, K. Ichiyanagi, M. Tanoue, and R. Suwarman, "Observational research on stable isotopes in precipitation over Indonesian maritime continent," *Nihon Suimon Kagaku Kaishi (Online)*, vol. 46, no. 1, pp. 7–28, 2016.

[47] H. A. Belgaman, K. Ichiyanagi, R. Suwarman, M. Tanoue, E. Aldrian, A. I. D. Utami, and S. D. A. Kusumaningtyas, "Characteristics of seasonal precipitation isotope variability in Indonesia," *Hydrological Research Letters*, vol. 11, no. 2, pp. 92–98, 2017.

[48] J. Perkel, "Democratic databases: science on GitHub," *Nature*, vol. 538, no. 7623, pp. 127–128, 2016.

[49] P. Wessel, J. F. Luis, L. Uieda, R. Scharroo, F. Wobbe, W. H. F. Smith, and D. Tian, "The Generic Mapping Tools Version 6," *Geochemistry, Geophysics, Geosystems*, vol. 20, no. 11, pp. 5556–5564, 2019.

[50] L. Uieda, D. Tian, W. J. Leong, W. Schlitzer, M. Grund, M. Jones, Y. Fröhlich, L. Toney, J. Yao, Y. Magen, J.-H. Tong, K. Materna, A. Belem, T. Newton, A. Anant, M. Ziebarth, J. Quinn, and P. Wessel, "PyGMT: A Python interface for the Generic Mapping Tools," 2023. Software available from `https://doi.org/10.5281/zenodo.7772533`.

[51] S. De Graaf, H. B. Vonhof, T. Weissbach, J. A. Wassenburg, E. J. Levy, T. Kluge, and G. H. Haug, "A comparison of isotope ratio mass spectrometry and cavity ring-down spectroscopy techniques for isotope analysis of fluid inclusion water," *Rapid Communications in Mass Spectrometry*, vol. 34, no. 16, p. e8837, 2020.

[52] S. Maithani and M. Pradhan, "Cavity ring-down spectroscopy and its applications to environmental, chemical and biomedical systems," *Journal of Chemical Sciences*, vol. 132, pp. 1–19, 2020.

[53] H. Sagayama, N. M. Racine, T. C. Shriver, and D. A. Schoeller, "Comparison of isotope ratio mass spectrometry and cavity ring-down spectroscopy procedures and precision of the doubly labeled water method in different physiological specimens," *Rapid Communications in Mass Spectrometry*, vol. 35, no. 21, p. e9188, 2021.

[54] J. A. Hutchings and B. L. Konecky, "Optimization of a Picarro L2140-i cavity ring-down spectrometer for routine measurement of triple oxygen isotope ratios in meteoric waters," *Atmospheric Measurement Techniques*, vol. 16, no. 6, pp. 1663–1682, 2023.

[55] J. Zhang and Z. Xu, "Vacuum extraction of high-salinity water for the determination of oxygen and hydrogen isotopic compositions using cavity ring-down spectroscopy," *Microchemical Journal*, vol. 190, p. 108678, 2023.

[56] G. M. Hornberger, "New manuscript guidelines for the reporting of stable hydrogen, carbon, and oxygen isotope ratio data," *Water Resources Research*, vol. 31, no. 12, pp. 2895–2895, 1995.

[57] T. B. Coplen, "Normalization of oxygen and hydrogen isotope data," *Chemical Geology: Isotope Geoscience Section*, vol. 72, no. 4, pp. 293–297, 1988.

[58] D. Taylor, "Work the shell: analyzing comma-separated values (csv) files," *Linux Journal*, vol. 2015, no. 260, p. 3, 2015.

[59] S. Mäs, D. Henzen, L. Bernard, M. Müller, S. Jirka, and I. Senner, "Generic schema descriptions for comma-separated values files of environmental data," in *The 21th AGILE International Conference on Geographic Information Science*, 2018.

[60] H. Craig, "Isotopic variations in meteoric waters," *Science*, vol. 133, no. 3465, pp. 1702–1703, 1961.

[61] L. Merlivat and J. Jouzel, "Global climatic interpretation of the deuterium-oxygen 18 relationship for precipitation," *Journal of Geophysical Research: Oceans*, vol. 84, no. C8, pp. 5029–5033, 1979.

[62] S. Pfahl and H. Sodemann, "What controls deuterium excess in global precipitation?," *Climate of the Past*, vol. 10, no. 2, pp. 771–781, 2014.

[63] R. Sánchez-Murillo, A. M. Durán-Quesada, C. Birkel, G. Esquivel-Hernández, and J. Boll, "Tropical precipitation anomalies and d-excess evolution during El Niño 2014-16," *Hydrological Processes*, vol. 31, no. 4, pp. 956–967, 2017.

[64] K. Yoshikawa, J. Úbeda, P. Masías, W. Pari, F. Apaza, P. Vasquez, B. Ccallata, R. Concha, G. Luna, J. Iparraguirre, *et al.*, "Current thermal state of permafrost in the southern Peruvian Andes and potential impact from El Niño–Southern Oscillation (ENSO)," *Permafrost and Periglacial Processes*, vol. 31, no. 4, pp. 598–609, 2020.

[65] L. Shao, L. Tian, Z. Cai, C. Wang, and Y. Li, "Large-scale atmospheric circulation influences the ice core d-excess record from the central Tibetan Plateau," *Climate Dynamics*, vol. 57, no. 7-8, pp. 1805–1816, 2021.

[66] S. Van Der Walt, S. C. Colbert, and G. Varoquaux, "The NumPy array: a structure for efficient numerical computation," *Computing in science & engineering*, vol. 13, no. 2, pp. 22–30, 2011.

[67] W. McKinney *et al.*, "pandas: a foundational Python library for data analysis and statistics," *Python for high performance and scientific computing*, vol. 14, no. 9, pp. 1–9, 2011.

[68] K. Rozanski, L. Araguás-Araguás, and R. Gonfiantini, "Isotopic patterns in modern global precipitation," *Climate change in continental isotopic records*, vol. 78, pp. 1–36, 1993.

[69] A. L. Putman, R. P. Fiorella, G. J. Bowen, and Z. Cai, "A global perspective on local meteoric water lines: Meta-analytic insight into fundamental controls and practical constraints," *Water Resources Research*, vol. 55, no. 8, pp. 6896–6910, 2019.

[70] L. N. Arellano, S. P. Good, R. Sánchez-Murillo, W. T. Jarvis, D. C. Noone, and C. E. Finkenbiner, "Bayesian estimates of the mean recharge elevations of water sources in the Central America region using stable water isotopes," *Journal of Hydrology: Regional Studies*, vol. 32, p. 100739, 2020.

[71] J. A. Torres-Martínez, A. Mora, P. S. K. Knappett, N. Ornelas-Soto, and J. Mahlknecht, "Tracking nitrate and sulfate sources in groundwater of an urbanized valley using a multi-tracer approach combined with a bayesian isotope mixing model," *Water Research*, vol. 182, p. 115962, 2020.

[72] Q. Zhang, H. Wang, and C. Lu, "Tracing sulfate origin and transformation in an area with multiple sources of pollution in northern China by using environmental isotopes and Bayesian isotope mixing model," *Environmental Pollution*, vol. 265, p. 115105, 2020.

[73] X. Kang, Y. Niu, H. Yu, P. Gou, Q. Hou, X. Lu, and Y. Wu, "Effect of rainfall-runoff process on sources and transformations of nitrate using a combined approach of dual isotopes, hydrochemical and Bayesian model in the Dagang River basin," *Science of the Total Environment*, vol. 837, p. 155674, 2022.

[74] A. Zaryab, H. R. Nassery, K. Knoeller, F. Alijani, and E. Minet, "Determining nitrate pollution sources in the Kabul Plain aquifer (Afghanistan) using stable isotopes and Bayesian stable isotope mixing model," *Science of the Total Environment*, vol. 823, p. 153749, 2022.

[75] H. Mao, C. Wang, S. Qu, F. Liao, G. Wang, and Z. Shi, "Source and evolution of sulfate in the multilayer groundwater system in an abandoned mine—Insight from stable isotopes and Bayesian isotope mixing model," *Science of the Total Environment*, vol. 859, p. 160368, 2023.

[76] K. Klauenberg, G. Wübbeler, B. Mickan, P. Harris, and C. Elster, "A tutorial on Bayesian normal linear regression," *Metrologia*, vol. 52, no. 6, p. 878, 2015.

[77] M. West, "Outlier models and prior distributions in Bayesian linear regression," *Journal of the Royal Statistical Society Series B: Statistical Methodology*, vol. 46, no. 3, pp. 431–439, 1984.

[78] G. L. Jones and Q. Qin, "Markov chain Monte Carlo in practice," *Annual Review of Statistics and Its Application*, vol. 9, pp. 557–578, 2022.

[79] N. Metropolis, A. W. Rosenbluth, M. N. Rosenbluth, A. H. Teller, and E. Teller, "Equation of state calculations by fast computing machines," *The Journal of Chemical Physics*, vol. 21, no. 6, pp. 1087–1092, 1953.

[80] W. K. Hastings, "Monte Carlo sampling methods using Markov chains and their applications," *Biometrika*, vol. 57, no. 1, pp. 97–109, 1970.

[81] S. Chib and E. Greenberg, “Understanding the Metropolis-Hastings Algorithm,” *The american statistician*, vol. 49, no. 4, pp. 327–335, 1995.

[82] Y. Fan, X. Shi, Q. Duan, and L. Yu, “Towards reliable uncertainty quantification for hydrologic predictions, Part I: Development of a particle copula Metropolis Hastings method,” *Journal of Hydrology*, vol. 612, p. 128163, 2022.

[83] S. Herho, F. Fajary, and D. Irawan, “On the Statistical Learning Analysis of Rain Gauge Data over the Natuna Islands,” *Indonesian Journal of Statistics and Its Applications*, vol. 6, no. 2, pp. 347–357, 2022.

[84] S. H. S. Herho, “A Univariate Extreme Value Analysis and Change Point Detection of Monthly Discharge in Kali Kupang, Central Java, Indonesia,” *JOIV: International Journal on Informatics Visualization*, vol. 6, no. 4, pp. 862–868, 2022.

[85] S. Sharma and P. P. Mujumdar, “Modeling concurrent hydroclimatic extremes with parametric multivariate extreme value models,” *Water Resources Research*, vol. 58, no. 2, p. e2021WR031519, 2022.

[86] R. Vinnarasi and C. T. Dhanya, “Time-varying Intensity-Duration-Frequency relationship through climate-informed covariates,” *Journal of Hydrology*, vol. 604, p. 127178, 2022.

[87] H. Xu, S. Song, T. Guo, and H. Wang, “Two-stage hybrid model for hydrological series prediction based on a new method of partitioning datasets,” *Journal of Hydrology*, vol. 612, p. 128122, 2022.

[88] B. Zolghadr-Asli, O. Bozorg-Haddad, M. Enayati, and H. A. Loáiciga, “Sensitivity of non-conditional climatic variables to climate-change deep uncertainty using Markov Chain Monte Carlo simulation,” *Scientific Reports*, vol. 12, no. 1, p. 1813, 2022.

[89] L. F. South, M. Riabiz, O. Teymur, and C. J. Oates, “Postprocessing of MCMC,” *Annual Review of Statistics and Its Application*, vol. 9, pp. 529–555, 2022.

[90] C. Karras, A. Karras, M. Avlonitis, and S. Sioutas, “An overview of mcmc methods: From theory to applications,” in *IFIP International Conference on Artificial Intelligence Applications and Innovations*, pp. 319–332, Springer, 2022.

[91] S. Agrawal, D. Vats, K. Łatuszyński, and G. O. Roberts, “Optimal scaling of MCMC beyond Metropolis,” *Advances in Applied Probability*, vol. 55, no. 2, pp. 492–509, 2023.

[92] J. Salvatier, T. V. Wiecki, and C. Fonnesbeck, “Probabilistic programming in Python using PyMC3,” *PeerJ Computer Science*, vol. 2, p. e55, 2016.

[93] Supari, F. Tangang, E. Salimun, E. Aldrian, A. Sopaheluwakan, and L. Juneng, “ENSO modulation of seasonal rainfall and extremes in Indonesia,” *Climate Dynamics*, vol. 51, pp. 2559–2580, 2018.

[94] T. Ferijal, O. Batelaan, and M. Shanafield, “Spatial and temporal variation in rainy season droughts in the Indonesian Maritime Continent,” *Journal of Hydrology*, vol. 603, p. 126999, 2021.

[95] S. He, N. F. Goodkin, D. Jackisch, M. R. Ong, and D. Samanta, “Continuous real-time analysis of the isotopic composition of precipitation during tropical rain events: Insights into tropical convection,” *Hydrological Processes*, vol. 32, no. 11, pp. 1531–1545, 2018.

[96] S. He, N. F. Goodkin, N. Kurita, X. Wang, and C. M. Rubin, “Stable isotopes of precipitation during tropical Sumatra Squalls in Singapore,” *Journal of Geophysical Research: Atmospheres*, vol. 123, no. 7, pp. 3812–3829, 2018.

[97] C. Funk, P. Peterson, M. Landsfeld, D. Pedreros, J. Verdin, S. Shukla, G. Husak, J. Rowland, L. Harrison, A. Hoell, *et al.*, “The climate hazards infrared precipitation with stations—a new environmental record for monitoring extremes,” *Scientific data*, vol. 2, no. 1, pp. 1–21, 2015.

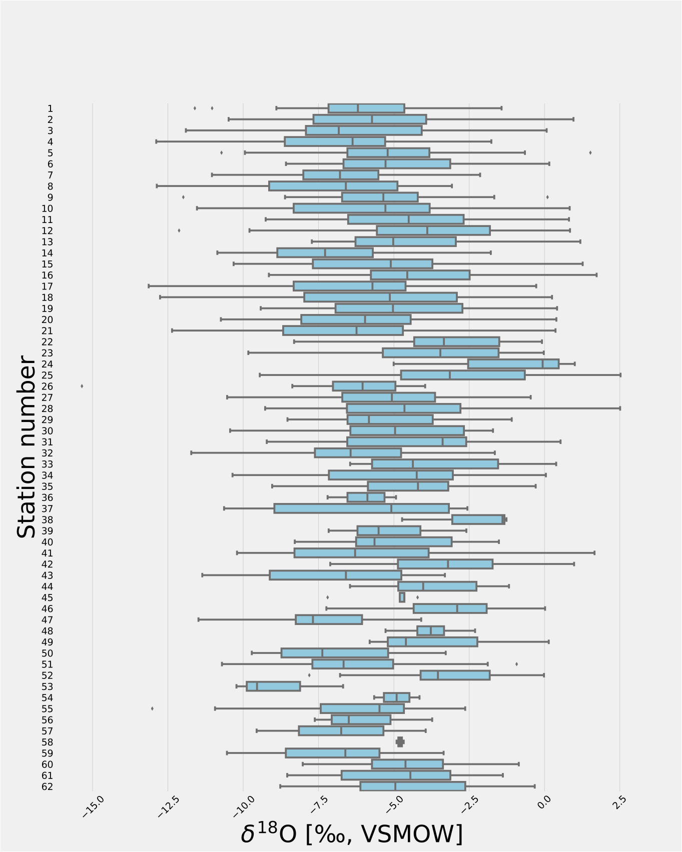

(a)

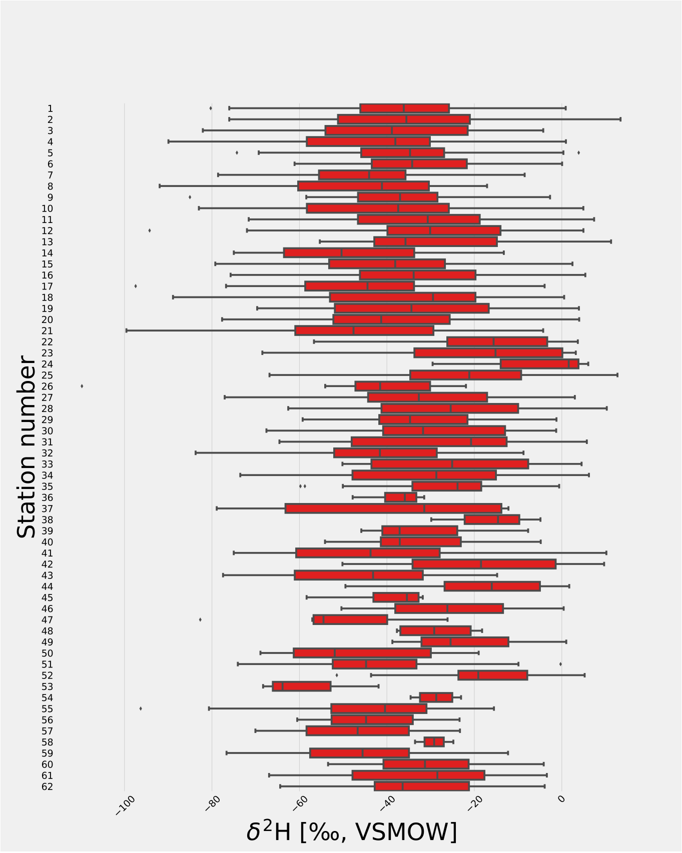

(b)

Figure 3: Box plots of the monthly (a) δ^{18}O and (b) δ^2H recorded by the 62 stations between September 2010 and September 2017.

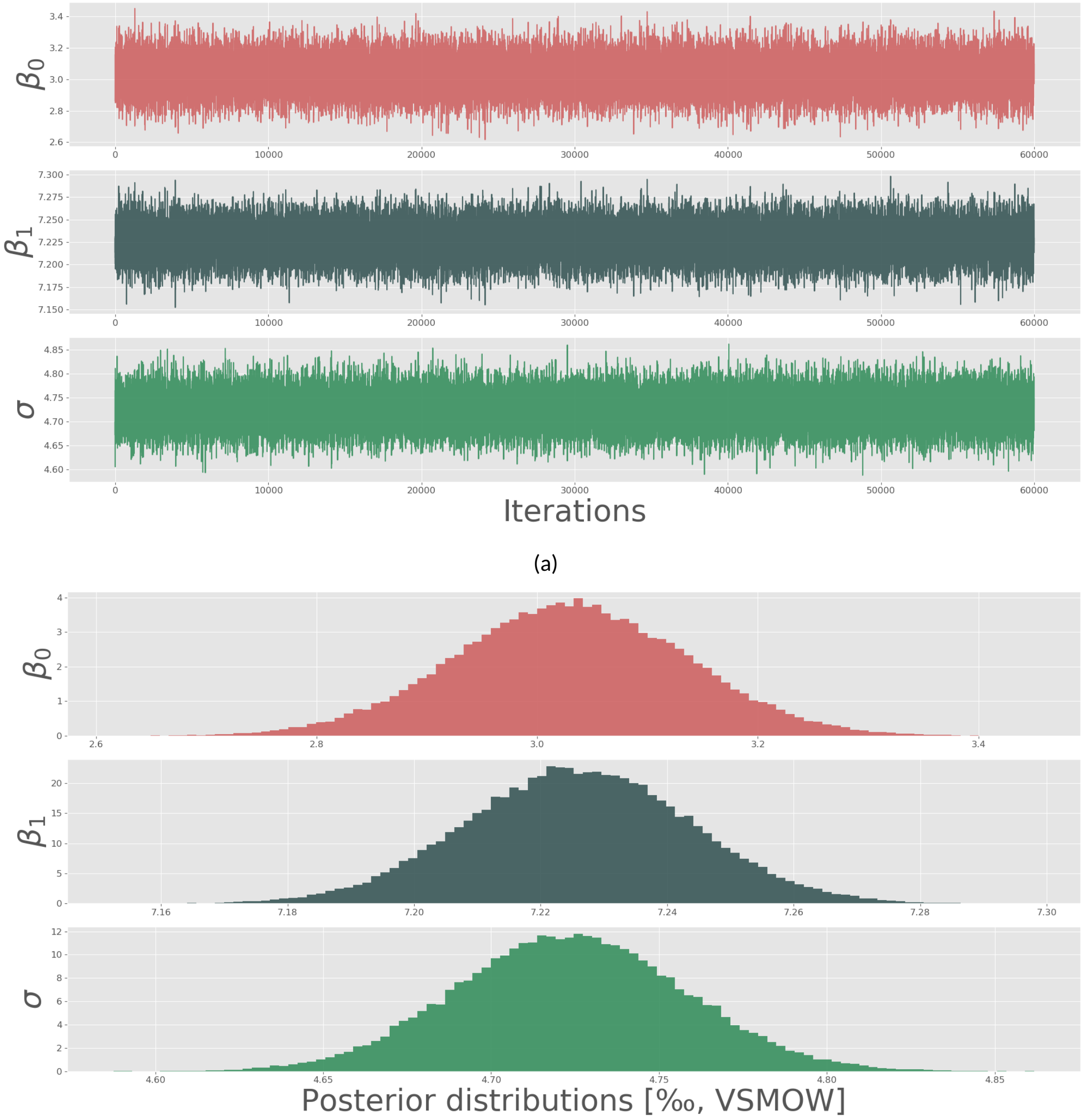

(a)

(b)

Figure 4: (a) BLR posterior parameter trace plots for the intercept (upper panel), slope (middle panel), and standard deviation (lower panel). (b) Posterior distribution of the three linear regression parameters: intercept (upper panel), slope (middle panel), and standard deviation (lower panel).

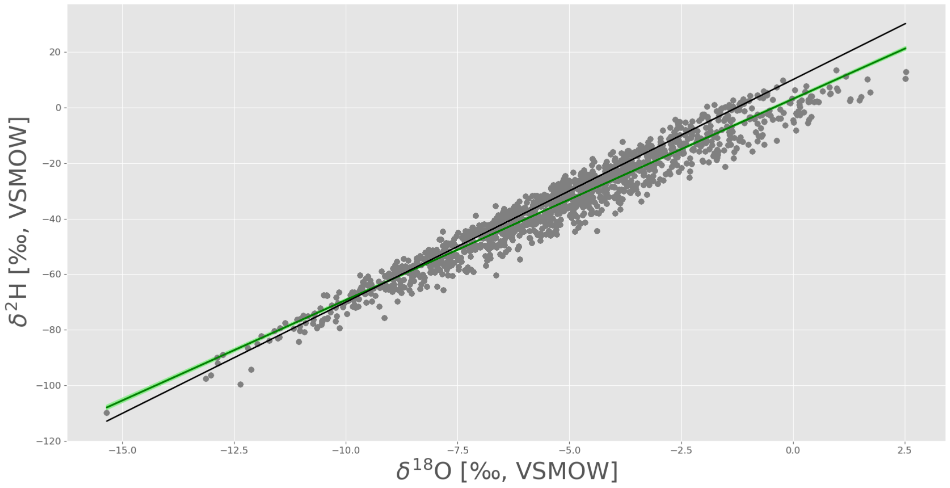

Figure 5: The GMWL (solid black line) compared to the LMWL (the posterior mean shown by a solid green line, light green area shows 95% credible interval obtained from the highest posterior density interval (HPDI)) of all stations over the IMC. Grey dots indicate individual data points.